Electronic Supplementary Material (ESI) for Dalton Transactions.

Fabrication of RGD-conjugated $Gd(OH)_3$:Eu Nanorods with Enhancement of Magnetic Resonance, Luminescence Imaging and *In vivo* Tumor Targeting

Bianyun Cai[a], Zhongbing Huang[a]*, Zhi Wu[a], Lei Wang[b], Guangfu Yin[a], Fabao Gao[b]*

a. College of Materials Science and Engineering, Sichuan University, Chengdu, 610065, China

Tel: 86-28-85413003. Fax: 86-28-85413003.

Email: zbhuang@scu.edu.cn

Address: No.24, South 1st Section, 1st Ring Road, Chengdu, 610065, China

b. Molecular Imaging Center, Department of Radiology, West China Hospital of Sichuan University,

Address: No.2, 4th Keyuan Road, Chengdu, 610093, China.

Email: gaofabao@yahoo.com; Fax: 86-28-85164081; Tel: 86-28-85164081.

1. Experimental section

1.1 Reagents and Materials

Gadolinium nitrate hexahydrate ($Gd(NO_3)_3 \cdot 6H_2O$) (99.99%), europium nitrate hexahydrate ($Eu(NO_3)_3 \cdot 6H_2O$) (99.99%) and 3-aminopropyl triethoxysilane (APTES) were purchased from Best Reagent (Chengdu, China). NaOH, dimethylsulfoxide (DMSO) and tetrachloromethane (CCl_4) were purchased from Chengdu Kelong Chemical Reagent Company. Maleimide and succinimide modified polyethylene glycol (Mal-PEG-NHS, M_w=5000 Da) was purchased from Jenkem Technology Co., Ltd. The thiolated cyclic Arg-Gly-Asp (cRGD-SH, M_w=594.65, pl=5.9) was purchased from GL Biochem (Shanghai, China). Trypsin, Dulbecco's modified Eagle's medium (DMEM), and fetal bovine serum (FBS) were purchased from Gibco (Gaithersberg, MD, USA). 3-(4,5-dimethylthiazol-2-yl)-2,5-diphenyl-tetrazolium bromide (MTT) was obtained from Sigma (St Louis, MO,USA). All chemical agents were of analytical grade and used directly without further purification. Fibroblast cells (L929), human umbilical vein endothelial cells (HUVEC) and human glioma (U251) cells were purchased from Shanghai Institute of Biochemical and Cell Biology.

1.2 Characterization

X-ray diffraction patterns (XRD) of the as-synthesized samples were analyzed with DX-1000 diffractometer (Dandong Fangyuan Instrument Co. Ltd, Cu Kα radiation, λ= 1.5418 Å, 40 kV, 80 mA) with step size of 0.06^o. The morphology of synthesized NRs was observed with scanning electron microscopy (SEM, JEOL–5900LV, 20 kV, Japan) and transmission electron microscopy (TEM, JEOL JEM-100CX, Japan). The shapes, crystalline structures and elements contents of the samples were evaluated by high-resolution transmission emission microscopy (HRTEM, JEOL-2000, 200 kV, Japan), HRTEM (Libra 200FE, Carl Zeiss SMT Pte Ltd) equipped with energy dispersive x-ray spectrum (EDX Oxford IETEM100). Thermogravimetry (TG) and differential scanning calorimetry (DSC) were carried out with a TG/SDTA851^e analyzer of METTLER-TOLEDO Co. Switzerland at a heating rate of 10 $^oC\ min^{-1}$ in alumina sample holder with alumina as a reference sample in air.

The magnetic property of samples was investigated by vibrating sample

magnetometer (VSM, Lake shore-7400, USA) with a step size of 1.42 cm^{-1}. The photoluminescence (PL) properties were investigated using the F-7000 FL Spectrophotometer with excitation at 395 nm. The luminescent images were obtained with a CONON 750D digital camera. The Ultraviolet spectrum (UV) was obtained by UV-vis absorption spectroscopy (U-3010, Hitachi Ltd). Fourier transform infrared (FT-IR) spectra were recorded with a Thermo Nicolet Smart-380 FT-IR spectrometer in the frequency range 400-4000 cm^{-1} at room temperature. The Zeta-potential of NRs was measured with dynamic light scattering using a Malvern Nano Series ZS particle size analyzer (Worcestershire, UK, USA). Inductively coupled plasma atomic emission spectroscopy (ICP-AES) was used to measure NRs concentrations in various solutions at each stage of NRs experiments, including bio-conjugations, in vitro cell uptake experiments and in vivo test.

1.3 Release of Gd ions from NRs in vitro

In order to evaluate the effect of PEG coating on the degradation of NRs, the $Gd(OH)_3$:Eu NRs and PEG-NRs were immersed in newborn calf serum (NCS) for different time. After NRs were immersed in NCS for 1~10 d, the degradation ratio of NRs could be obtained by measuring the resealed Gd^{3+} concentration from NRs into NCS and calculating the degraded amount of NRs. Samples of the released Gd^{3+} were prepared as following: 20 mg NRs were immersed in 20 mL NCS at 37 ℃. After 1, 3, 5, 7 and 10 days, 2 mL supernatants were collected, respectively. The supernatants were boiled in a digestion solution containing mixed acids (nitric acid : perchloric acid, v : v = 3: 1) for 30 min. The concentrations of released Gd^{3+} were obtained by inductively coupled plasma atomic emission spectroscopy (ICP-AES, SPECTRO ARCOS, Germany), and the degradation ratio (%) = the amount of degraded NRs/the amount of NRs added into NCS.

1.4 In vitro hemolysis assay

The hemolysis assay experiments were carried out to evaluate the blood compatibility of the as-prepared NRs. Blood samples stabilized by EDTA were collected from mice heart. First, 1 mL of blood sample was added into 2 mL of PBS, and then red blood cells (RBCs) were isolated from serum by centrifugation at 8000 rpm for 10 min. After washed five times with 5 mL of PBS solution, RBCs were dispersed PBS solution till 1/10 of its

volume. 0.2 mL of diluted RBCs suspension was then mixed with (a) 0.8 mL of PBS as a negative control, (b) 0.8 mL of double-distilled water (D.I. water) as a positive control, and (c) 0.8 mL $Gd(OH)_3$:Eu NRs and PEG-NRs suspensions at concentrations ranging from 0 to 1000 μg mL^{-1}. Then all the mixtures were oscillated and kept at room temperature for 3 h. Finally, the mixtures were centrifuged at 12,000 rpm for 5 min, the absorbance of supernatants at 541 nm was determined by a Micro Plate Reader 3550 (Bio-Rad). The percent hemolysis of RBCs was calculated as following: percent hemolysis = [(sample absorbance – negative control absorbance) / (positive control hemolysis – negative control absorbance)] × 100%.

1.5 ROS generation

As reported, high level of intracellular reactive oxygen species (ROS) could affect cell viability.[1] L929 cells were planted into 12-well plate as described below. After cells were treated with the as-prepared NRs ($Gd(OH)_3$:Eu NRs and PEG-NRs) for 24 h, the intracellular ROS was quantitatively analyzed using enzyme linked immunosorbent assay (ELISA kit, R&D, USA). The absorbance was measured at 450 nm using Microplate Reader 3550 (Bio-Rad). The analysis process follows the ELISA kit instruction.

In the test of ROS generation, *in vitro* hemolysis assay and the affinity assay, we only checked for the difference between $Gd(OH)_3$:Eu NRs and PEG-NRs, but not for RGD-NRs because the cladding of PEG molecules was mainly used for increasing the water-solubility, cyto-compatibility and the blood circulation time of PEG-NRs, while the conjugation of cRGD was primarily used to improve the gliomas targeting property of those NRs. Besides, cRGD was micromolecule short peptide, which influence was negligible compared with macromolecular PEG (molecular weight is 5000).

1.6 Cell viability assay-MTT

L929 fibroblast cell line, human umbilical vein endothelial cell line (HUVEC), and U251 cell line were cultured in Dulbecco's modified Eagle's medium (DMEM, Gibco) supplemented with 10% fetal bovine serum (Gibco, BRL), 1 mM $_L$-glutamina, penicillin (20000 U/mL), and streptomycin (20000 U/mL), under a CO_2 (5%) atmosphere and at 37 ˚C. MTT assays of L929, HUVEC and U251 were used to evaluate the cyto-compatibility of $Gd(OH)_3$:Eu NRs and RGD-NRs, respectively. 100 μL of cells were seeded in 96-well plate at a density of 1×10^4 cells·mL^{-1}. Different concentrations of as-prepared NRs (25 ~

200 μg·mL^{-1}) were added into the culture wells, respectively, until the cells reached confluence. The media were removed after 24 h, cells were washed three times with PBS (pH = 7.4), the pictures of cells were obtained under the inverted fluorescence microscopy (IFM, IX-71, Olympus) at a magnification of 200 ×. Then 5 mg·mL^{-1} MTT (3-(4, 5-dimethylthiazol-2-yl)-2, 5 - diphenyltetrazolium bromide) was added into each well and incubated for 4 h. The formazan product was dissolved in 150 μL DMSO for 10 min and the absorbance at 490 nm was measured with a Micro Plate Reader 3550 (Bio-Rad). In the experiment, pure cells without NRs were used as control group, and all experiments were performed in triplicate. The cell viability (%) = optical density (OD) of the treated cells/OD of the untreated cells.

1.7 TEM observation of U251 cells

Transmission electron microscope (TEM) was used to analyze the internalization of $Gd(OH)_3$:Eu NRs, PEG-NRs and RGD-NRs U251 cells, respectively. First, cells were co-cultured with $Gd(OH)_3$:Eu NRs, PEG-NRs or RGD-NRs at 37 ℃ for 24 h. Secondly, cells were collected in a centrifuge tube of 10 mL, then centrifuged for 10 min (1500 r/min) and washed 3 times with PBS. Thirdly, after about 0.5% glutaraldehyde was added slowly along the centrifuge tube wall, cells were kept for 30 min at 4 °C. Subsequently, cells were centrifuged for 15 min (13000 r/min), fixed with 3% glutaraldehyde, and then placed at 4 °C. Finally, re-fixation was carried out in 1 % osmium tetroxide. Then, cell samples were serially dehydrated with acetone solutions (30, 50, 70, 90, and 100%, respectively) at room temperature, and the fixed cells were subsequently embedded in Epon 812. The ultrathin sections of cells were obtained using a Leica Ultracut UCT ultramicrotome (MT-X; RMC Inc., Tucson, AZ). Thin sections (~ 60 nm thickness) were stained with lead citrate, then observed and imaged in the TEM (HITACHI-600 IV, 160 kV).

1.8 In vitro tumor targeting assay

100 μL of cells (HUVEC and U251) were seeded in 12-well plate at a density of 5 × 10^4 cells/well, respectively. 200 μg·mL^{-1} $Gd(OH)_3$:Eu NRs and RGD-NRs were added into the culture wells, respectively, until the cells reached confluence. The media were removed after 24 h, then cells were washed three times with PBS (pH = 7.4), and the cellular morphology were observed directly under inverted fluorescence microscope at a

magnification of 200 ×. Then, cells were digested by Tyrisin and collected into 10 mL centrifuge tube. 1 mL nitric acid was added into these collected cells to lyse them and release the metal ions of NRs. Finally, the concentration of Gd ions was quantified using ICP-AES. Pure cells without adding NRs were used as control group, and all experiments were performed in triplicate.

1.9 Long-term toxicity test

A certain amount of $Gd(OH)_3$:Eu NRs, PEG-NRs and RGD-NRs were dispersed in physiological saline to prepare into 1 mg/mL solution, respectively, and 200 μL of prepared solution was injected into Kunming mice (n=3) via the tail vein, and the Kunming mice with no NRs injection was selected as the control group. The body weights of the mice in all groups were recorded for 10 days, and 10 days later, the mice were sacrificed. Then, their heart, liver, spleen, lung and kidney were extracted and divided into two parts, respectively. One part was used to measure the *in vivo* bio-distribution of the NRs, and the other was conducted histology analysis.

1.10 In vitro and in vivo MR imaging

In vitro T_1-weighted MRI and relaxation time measure was performed with a 7.0 T MR imaging system (BioSpec, Bruker, Germany). The $Gd(OH)_3$:Eu NRs were dispersed into PBS solution containing 0.5% agarose with different concentrations (0.25 ~ 4.0 mM). Then these dispersions in 1.5 mL tubes were placed MRI system, respectively. T_1-weighted images and T_1 values were obtained by the multi-slice multi-echo sequence. The measurement conditions were as follows: a field of view (FOV) of 4 × 4 cm, a slice thickness of 2.0 mm, the number of excitations (NEX) of 4, the size of the images of 256 × 256, the value of repetition time (TR) of 180 ms, and echo time (TE) of 6.0 ms.

Male nude mice (18 ~ 22 g) were injected in the hip subcutaneous with 200 μL cell suspension of 4×10^6 U251 cell, then the tumor grew to about 300 mm^3 within 7 d. In order to analyze their contrast enhancement of *in vivo* MR imaging in tumor field, the three NRs ($Gd(OH)_3$:Eu NRs, PEG-NRs and RGD-NRs, respectively) were dispersed in 0.9 wt% NaCl solution, then 20 μL (1 mg/mL) suspensions were injected into mice through tail vein with 5 needle (0.5 mm diameter). After 3 and 24 h of post-injection, MR images were obtained in the 7.0 T MR imaging system according to the above measurement conditions, and the MR images of the mice pre-injected with NRs were used

as control groups. The brightness of tumor interior and tumor periphery in a serial of MRI images were measureed with the soft of Matlab 7.0 to obtain their average brightness ($V_{tumor\ interior}$ and $V_{tumor\ periphery}$, the tumor interior refers to the whole tumor and the edge of the tumor, while the tumor periphery refers to the muscle tissue around the tumor), and the contrast intensity (ΔV) was calculated accroding to $\Delta V = V_{tumor\ interior} - V_{tumor\ periphery}$.

1.11 Cellular luminescence imaging

U251 cells were planted in 6-well plate (BD Biosciences) to culture in DMEM, containing 10 % fetal bovine serum (FBS), 100 U/mL penicillin and 100 mg/mL streptomycin at 37 °C under 5 % CO_2 for 1 day, and cells were co-cultured with $Gd(OH)_3$:Eu NRs, PEG-NRs and RGD-NRs (200 μg/mL, dispersed in DMEM) for 1 day at 37 °C under 5 % CO_2, respectively. Then cells were successively fixed with 4 % paraformaldehyde for 10 ~ 15 min at 4 °C, and incubated with 4', 6-diamidino-2-phenyindole (DAPI, Sigma, 100μg/mL) for 5 min. After the incubation, cells were washed 3 times with PBS and observed under ultraviolet (UV) by IFM (IX-71, Olympus).

1.12 In vivo tests

Six-week old Kunming mice were purchased from the Dashuo laboratory animal Co. limited (Chengdu, China). Athymic female BALB/c nude mice, 4-6 weeks of age, were purchased from and fostered in the West China Medical Laboratory Animal Center (Chengdu, China). All animal procedures were in agreement with the guidelines of the Institutional Animal Care and Use Committee.

1.12.1 In vivo bio-distribution measurement

$Gd(OH)_3$:Eu NRs, PEG-NRs and RGD-NRs were dispersed in physiological saline to prepare 1 mg/mL solution, respectively, and 200 μL solution was injected into Kunming mice via the tail vein, and the Kunming mice without NRs injection were selected as the control group. Then mice were sacrificed 24 h after the injection, different organs (heart, liver, spleen, lung, kidney and tumor) were obtained and put separately into wide-mouth bottles. The collected organs were washed with physiological saline (0.9%) for several times to remove the residual blood (especially lungs). Then, the organs were digested in a digestion solution containing mixed acids (nitric acid: perchloric acid, v / v = 3 / 1) for over 30 min, until the transparent solutions appeared. The volume was set to 5 mL and the concentrations of Gd^{3+} were quantified with ICP-AES.

1.12.2 Histology analysis

For the histology analysis, mice were sacrificed after 24 h of administration. The tissues (heart, liver, spleen, lung and kidney) were collected from the above four groups ($Gd(OH)_3$:Eu NRs group, PEG-NRs group, RGD-NRs group and the control group) and fixed in 4 wt% paraformaldehyde solution (PBS, pH=7.4). Then, the collected tissues were embedded in paraffin, sectioned (4 μm of thickness), as well as stained with hematoxylin and eosin (H&E). The histological sections were observed under an optical microscopy (Nikon Eclipse Ti-S, CCD: Ril).

1.12.3 In vivo luminescence imaging

For *in vivo* luminescence imaging, tumor-bearing nude mice (TB-N mice) was administered with 0.9 wt% NaCl solution containing RGD-NRs (200 μL, 1 mg/mL) by subcutaneous tumor injection, which was denoted as the test group. Another nude mouse without injection was denoted as the control group. Before experiment, nude mice were first anesthetized by intraperitoneal injection of 10 wt% chloral hydrate. The *in vivo* luminescence imaging experiment was performed with a Maestro *in vivo* imaging system (Maestro EX, America) under the excitation of 500 nm at 4 h of post-injection.

1.13 Statistical analysis

The data were expressed as mean ± standard deviation of a representative of three similar experiments carried out in triplicate. Statistical analysis was carried out with the Statistical Package for Social Sciences (SPSS). LSD and Tukey tests were used to evaluate their differences between the test and the control groups, and we considered a p value of ≤ 0.05 as statistically significant.

1. Results and Discussion:

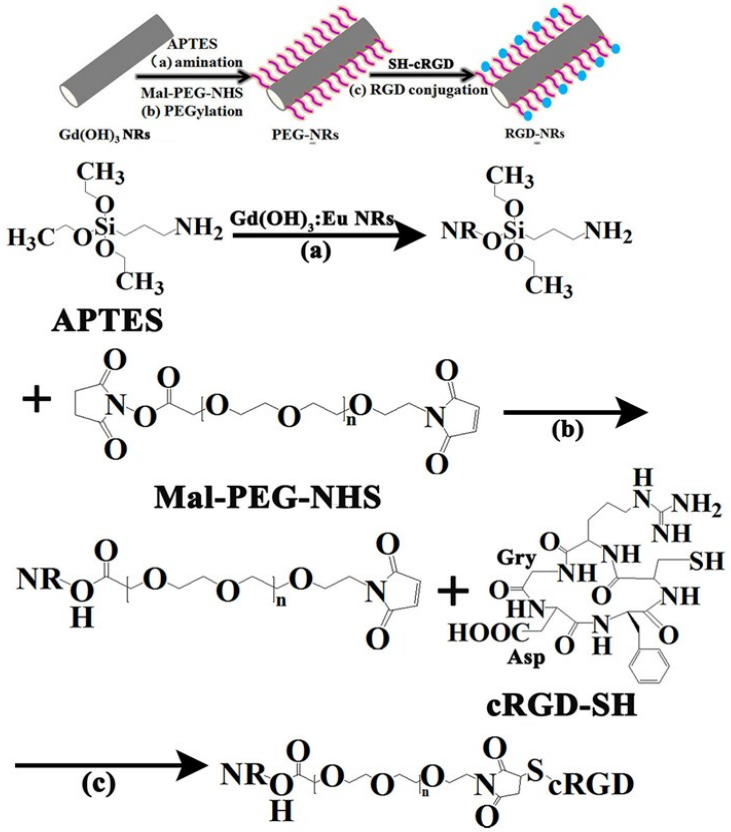

Scheme 1. The preparation schematic illustration of RGD-conjugated $Gd(OH)_3$:Eu NRs and the involved reactions.

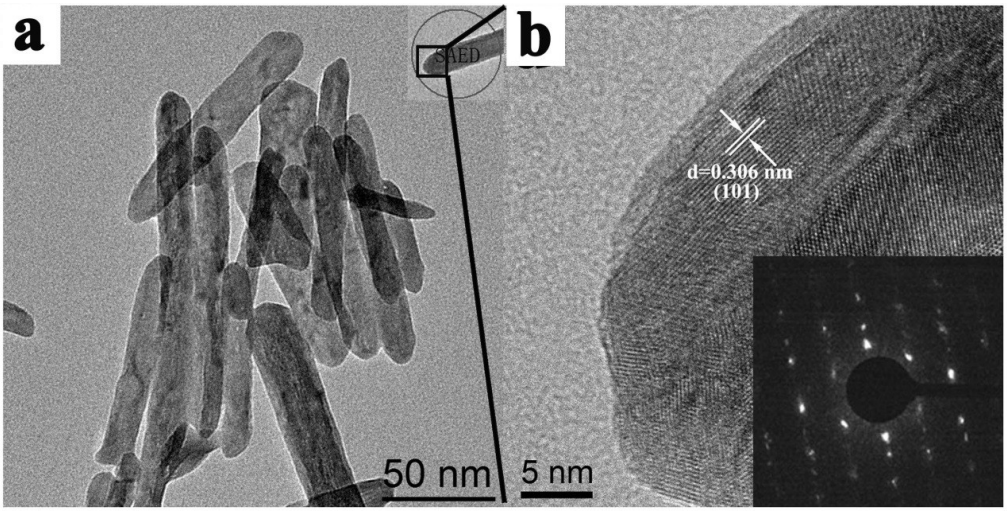

Fig. S1. The TEM image (a), HRTEM image and SAED image (b) of $Gd(OH)_3$:Eu NRs.

SEM images (Fig. S2) and TEM images (Fig. S3) of $Gd(OH)_3$ NRs with different percent of doped Eu showed that, with the increase of Eu content, particles with rod-like shape were observed. By calculating with software Image-Pro Plus 6.0, the size distribution obtained from SEM images was shown Table S1, it is found that, with the increase of Eu doping rate from 0 to 40%, although the average diameter of NRs was gradually and slightly increased, these NRs became shorter and coarser when the doping Eu rate changed from 0 % to 20 %, and NRs again became longer when the doping Eu rate increased to 30 % and 40 %. Furthermore, the size distribution obtained from about 150 NRs in TEM images of each samples were shown in Fig. S3, further confirm that the lengths of those NRs were first decreased with the increase of doped Eu to 20%, then increased with the increase of doped Eu to 40%, namely, the average length of NRs shows the similar change with the increase of doping Eu. This change of NRs length might be attributed to the fact that, due to the diameter of Eu ions is slightly smaller than that of Gd ions, the length of NRs doped with less Eu ions was changed smaller, however, the part NRs grew from the $Eu(OH)_3$ crystal nuclei when a number of Eu ions existed in reaction solution (such as 30%), leading to the increase of the average NRs length.

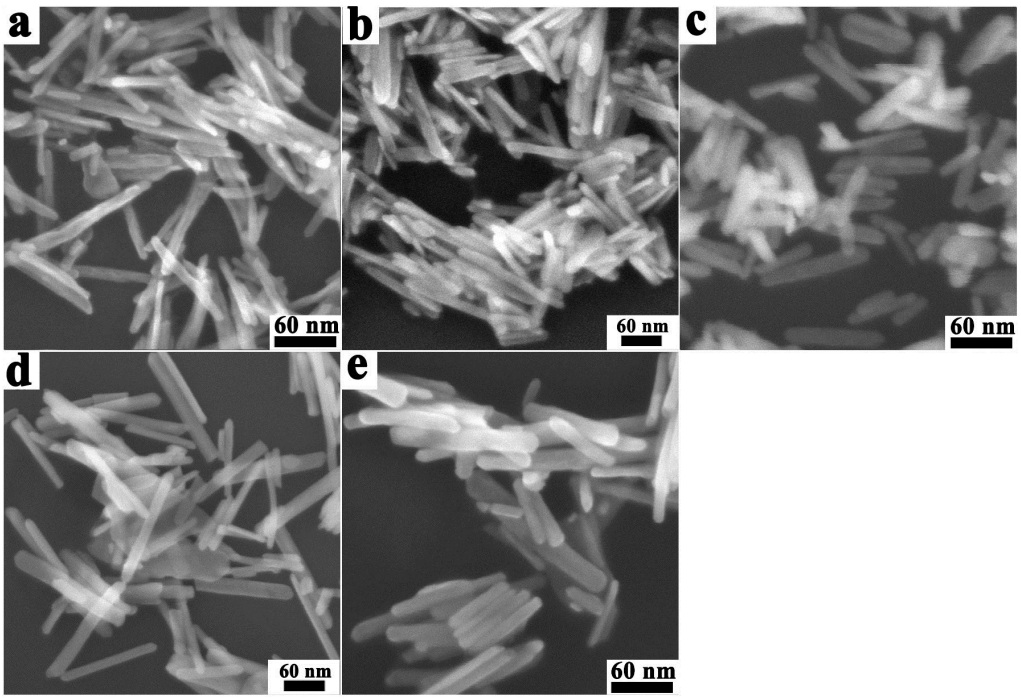

Fig. S2. SEM images of $Gd(OH)_3$ NRs with different percent of doped Eu (a) 0 %, (b) 10 %, (c) 20 %, (d) 30 %, (e) 40 %.

Table S1. The lengths and diameters of $Gd(OH)_3$ NRs with different Eu/Gd ratio (atomic %).

Eu content (%)	**0 %**	**10 %**	**20 %**	**30 %**	**40 %**
Length (nm)	118.3813	105.7839	85.1648	163.049	127.4659
SD	25.6473	30.4879	10.5599	30.5782	30.4915
Diameter (nm)	13.6839	14.2957	17.5789	19.0339	19.3132
SD	1.4863	1.5174	2.8718	2.7596	3.7869

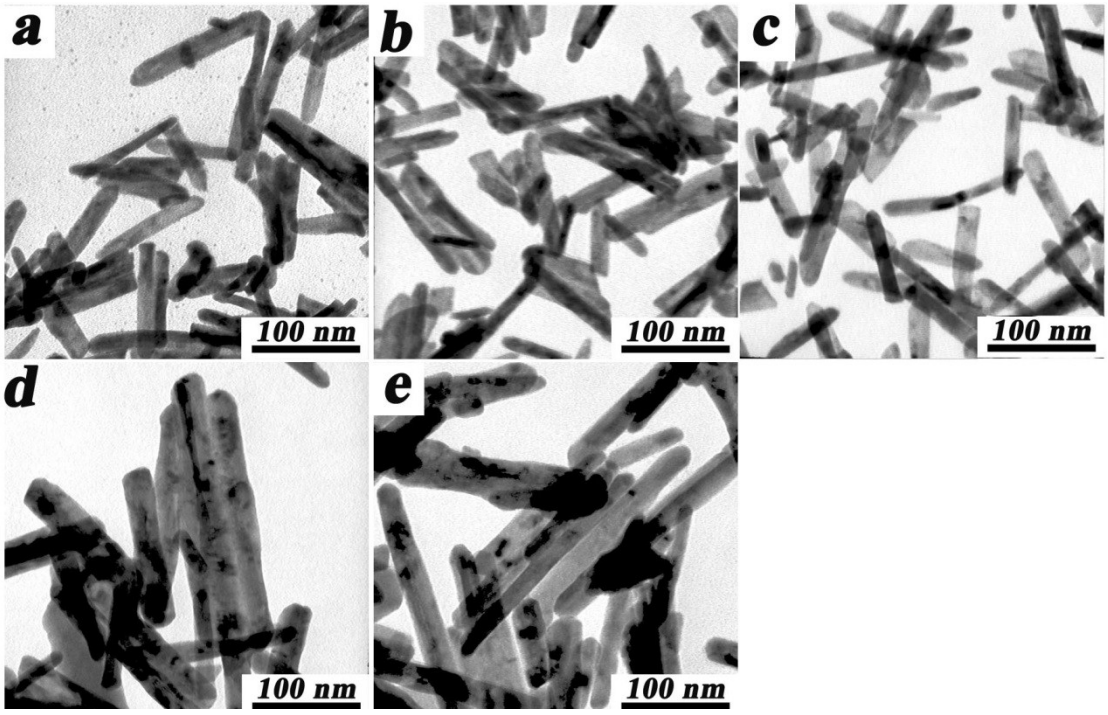

Fig. S3. TEM images of $Gd(OH)_3$ NRs with different percent of doped Eu (a) 0 %, (b) 10 %, (c) 20 %, (d) 30 %, (e) 40 %.

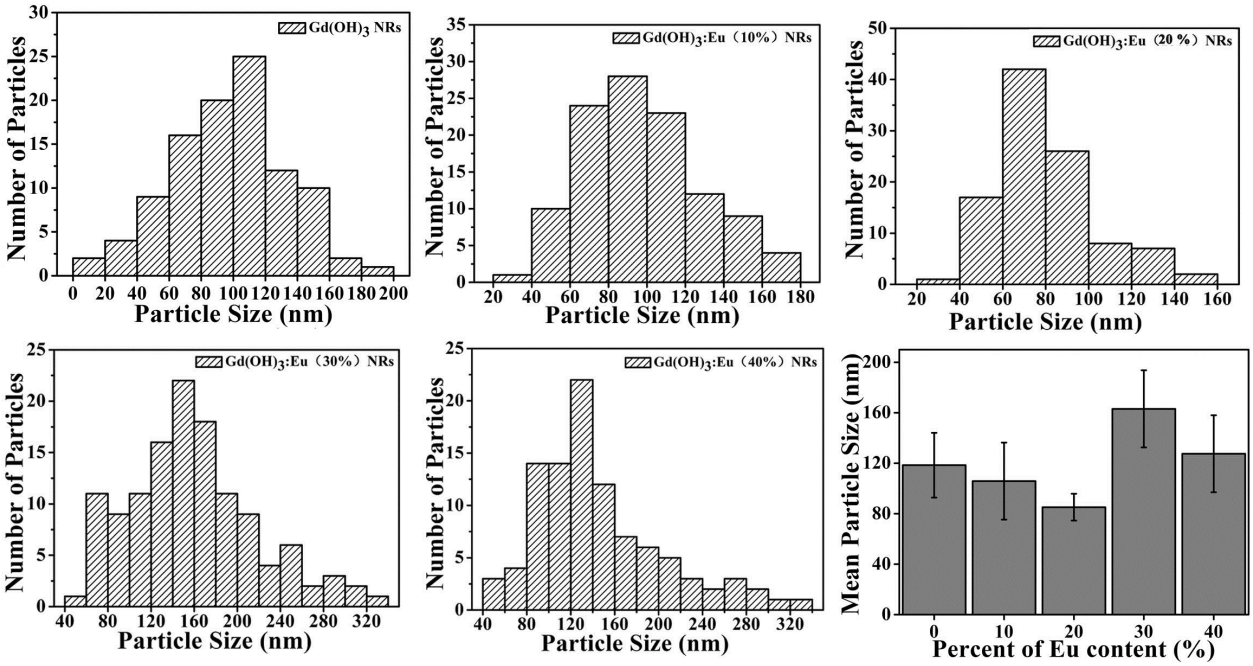

Fig. S4. The particle length distributions obtained from the TEM images: $Gd(OH)_3$ NRs with different percent of doped Eu (a) 0 %, (b) 10 %, (c) 20 %, (d) 30 %, (e) 40 %.

In Table S2, the results of energy dispersive x-ray spectrum (EDX) showed that the Eu/Gd ratio increased from 0.214 to 0.874 when the Eu rates in the reaction solutions were changed from 10 % to 40 %. Besides, the results showed that the oxygen content and the Gd +Eu content was approximately constant, and the slightly inconsistencies were inside the errors of the measurement.

Table S2. Element Contents of $Gd(OH)_3$ NRs in solutions with different Eu/Gd ratio (atomic %).

Element	0 %	10 %	20 %	30 %	40 %
O K	78.79±0.2	75.46±3.2	77.27±1.9	79.07±0.2	74.51±4.6
Eu L	0	4.42±1.3	5.94±0.8	7.65±0.1	11.88±2.7
Gd L	21.21±0.2	20.22±2.8	16.79±1.4	13.28±0.1	13.60±1.8
Total	100.0	100.0	100.0	100.0	100.0
Eu/Gd	0	0.214	0.354	0.576	0.874

Fig. S5 showed XRD patterns of $Gd(OH)_3$ and $Gd(OH)_3$:Eu NRs, which could be indexed as the hexagonal phase of $Gd(OH)_3$ (ICDD 00-083-2037), and the typical peaks of $Gd(OH)_3$:Eu (20% Eu) were slightly stronger than those of pure $Gd(OH)_3$. The crystallite sizes evaluated from the Sheller equation for $Gd(OH)_3$ and $Gd(OH)_3$:Eu were 16.0 nm and 18.9 nm, respectively, indicating that Eu doping could slightly improve the crystallite size of NRs.

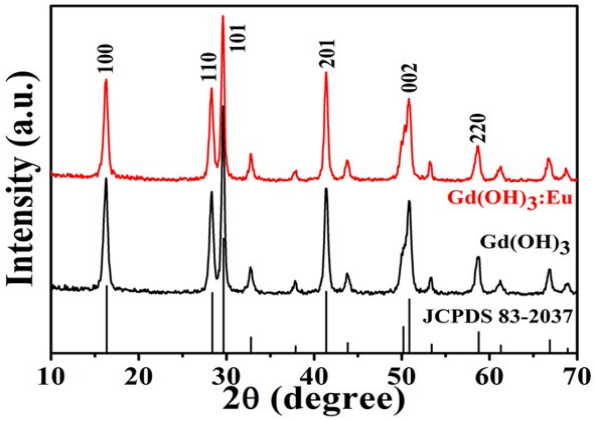

Fig. S5. The XRD patterns of the $Gd(OH)_3$ and $Gd(OH)_3$:Eu NRs.

Dynamic Light Scattering measurements provide with the hydrodynamic diameter and size distribution of the nanoparticles, which are also necessary to assess the degree of dispersion (or aggregation) of the particles. In Fig. S6, the hydrodynamic size of $Gd(OH)_3$:Eu NRs in alcohol was 189 nm by dynamic light scattering, which demonstrated the relatively good dispersion of those NRs.

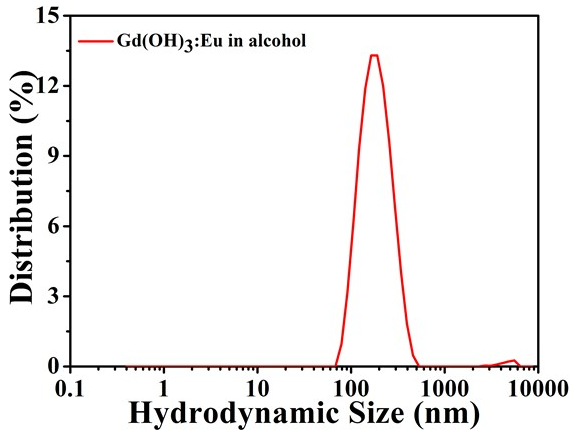

Fig. S6. Hydrodynamic size of $Gd(OH)_3$:Eu NRs dispersed in alcohol.

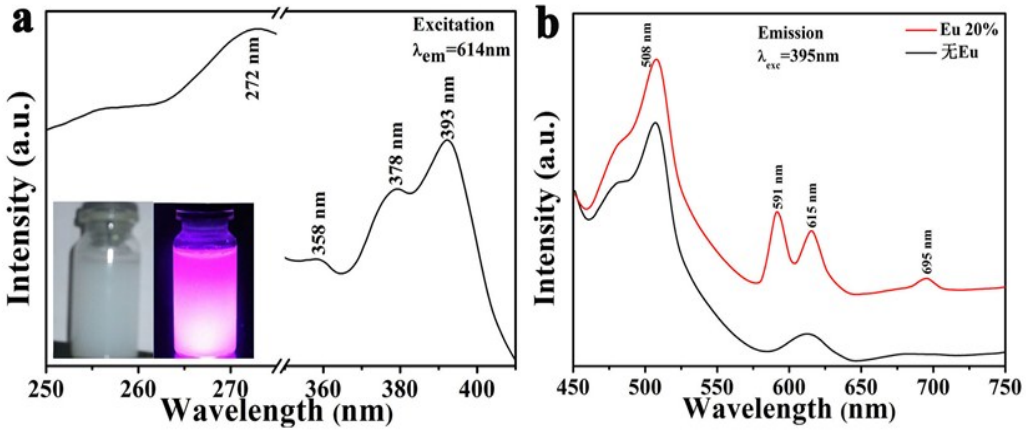

Fig. S7. The Excitation spectrum (a) and Emission spectra (b) of the prepared $Gd(OH)_3$ and $Gd(OH)_3$:Eu NRs, inset of (a) is the luminescent image and corresponding bright image of $Gd(OH)_3$:Eu NRs, and those NRs were dispersed in distilled water.

The relaxivity with the various Gd ions concentrations of $Gd(OH)_3$:Eu NRs with different Eu/Gd ratio were calculated from the slope of the concentration-dependent relaxation rate $1/T_1$ graph. In Fig. S8, it is found that the relaxivity of as-prepared NRs were reduced with the increase of Eu content. The lower r_1 value of the NRs with higher Eu content resulted from the concentration of Gd^{3+} in the NRs of the unit mass was decreased due to the doping of Eu^{3+}.

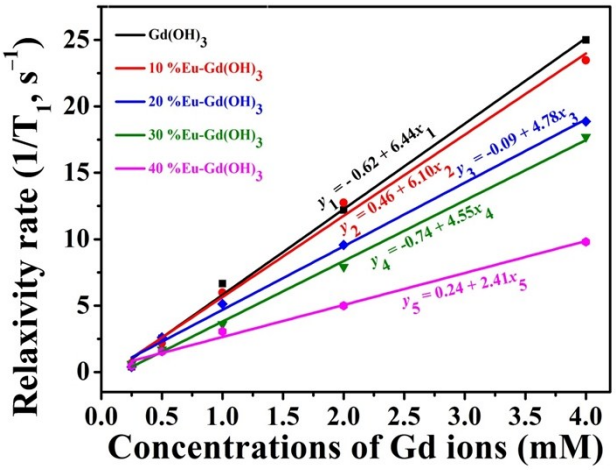

Fig. S8. The relaxation rate R_1 $(1/T_1)$ versus various Gd ions concentrations of $Gd(OH)_3$:Eu NRs with different Eu/Gd ratio.

Fig. S9 showed a series of T_1-weighted images of $Gd(OH)_3$:Eu NRs with different Eu/Gd ratio in the range of 0 ~ 4.0 mM Gd^{3+} in an agarose solution. With the increase of Gd^{3+} concentration, the T_1-weighted signal intensities were enhanced, leading to brighter images. However, the signal intensities were reduced with the increase of Eu content because of the lower r_1 value of those NRs with higher Eu content.

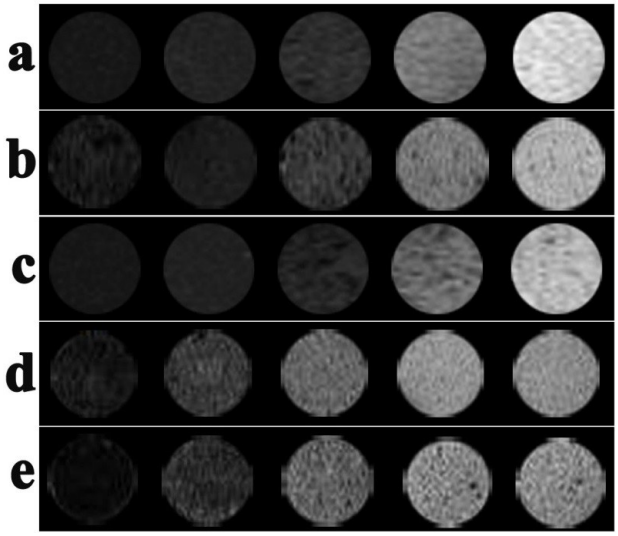

Fig. S9. T_1-weighted MR images of these NRs dispersed in agarose solution with various Gd ions concentrations: (a) $Gd(OH)_3$, (b) $Gd(OH)_3$:10% Eu, (c) $Gd(OH)_3$:20% Eu, (d) $Gd(OH)_3$:30% Eu and (e) $Gd(OH)_3$:40% Eu NRs.

Fig. S10 showed the luminescence images of the suspensions with Eu-doped $Gd(OH)_3$ NRs, exhibiting pink emission under ultraviolet light excitation of 395 nm. Besides, with the increase of Eu percentage in reaction solutions, the luminescent intensities of as-prepared NRs were enhanced. However, there was no significant difference of the pink luminescent intensities among 20 %, 30 % and 40 % of Eu content, which were all consistent with the results of emission spectra in Fig. S11.

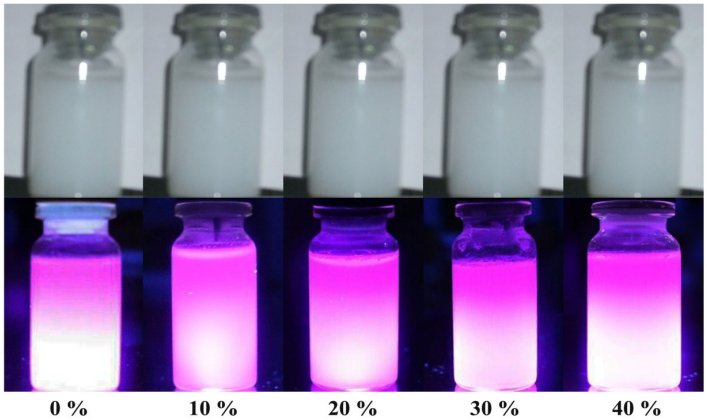

Fig. S10. Luminescent images and corresponding bright images of $Gd(OH)_3$ NRs in solutions with different Eu/Gd ratio, and NRs were dispersed in distilled water.

Fig. S11a showed the excitation spectrum of the Eu-doped $Gd(OH)_3$ (20% Eu content in the reactive metal ions) NRs monitored at the Eu^{3+} emission band (614 nm). A broad excitation band centered at 393 nm is observed, which was attributed to the f-f transitions of Eu^{3+}. Fig. S11b showed the emission spectra of $Gd(OH)_3$:Eu NRs, obtained at the different Eu content (0%, 10%, 20%, 30%, 40%, respectively) in the reactive metal ions. Upon the excitation of 395 nm, the single broad band with a maximum at 508 nm was ascribed to the charge transfer transition between the Eu-to-oxygen (Eu → O)[3]. The existence of Eu^{2+} might improve the relaxivity of $Gd(OH)_3$:Eu NRs, because Eu^{2+}/Eu^{3+} complexes could make contributions to redox responsive MR imaging.[1] The characteristic peaks at 591, 615 and 695 nm should correspond to $^5D_0 \rightarrow {}^7F_{1,2,4}$ energy level transitions of Eu^{3+}. With the increase of Eu doped in NRs (shown in Tab. S1), these typical peaks of Eu ions became gradually stronger. However, there was no significant difference of the characteristic peaks intensities among 20 %, 30 % and 40 % of Eu

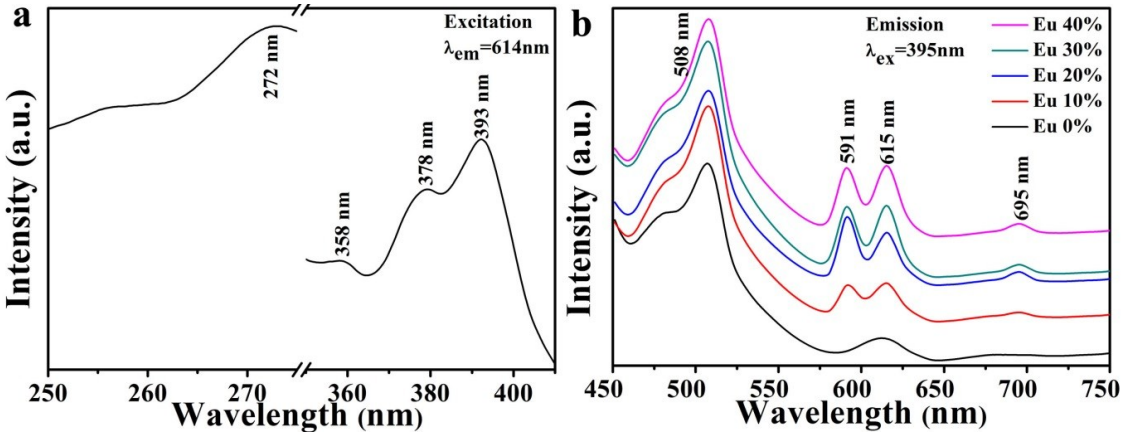

Fig. S11. Excitation spectrum (a) and Emission spectra (b) of the prepared $Gd(OH)_3$ NRs in solutions with different Eu/Gd ratio.

content.

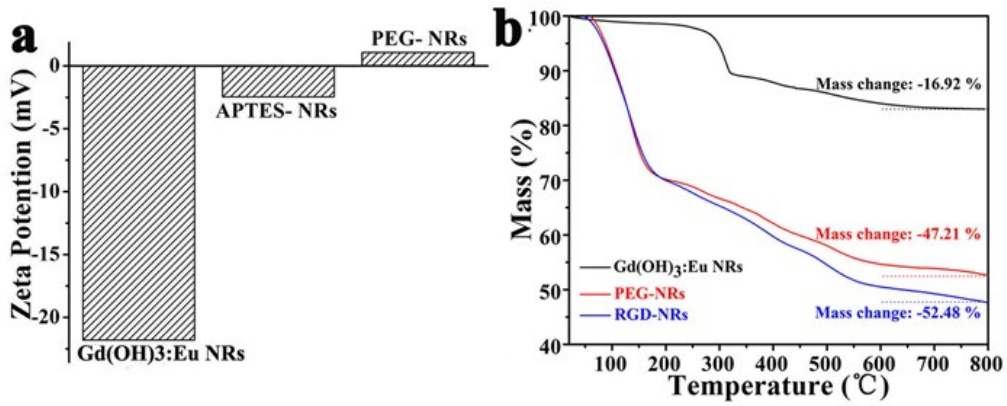

Fig. S12. (a) Zeta potential before and after the conjugation of hydrophilic dual-functional copolymer PEG, and the TG curves (b) in the temperature range from 20 to 800 °C of $Gd(OH)_3$:Eu NRs, PEG-NRs and RGD-NRs.

The affinity between newborn calf serum (NCS) and $Gd(OH)_3$:Eu NRs or PEG-NRs was analyzed via the contact angle measurement of wettability test. The better the wettability was, the smaller the contact angle would be, and the higher the affinity between NCS and NRs was. For each experiment, a single droplet of ~10 μL NCS was placed on the surface of NRs slices, then, the images were captured immediately. In Fig. S13, it was observed that the NCS droplet was nearly flat (contact angle was 18.75 °) on the surface of PEG-NRs, while the contact angle was significantly larger (~ 61°) on the surface of $Gd(OH)_3$:Eu NRs, indicating that the conjugation of PEG enhanced the affinity between NCS and NRs, thus increasing their blood circulation time and the efficiency of their internalization in targeted cells when these PEG-NRs were introduced *in vivo*.

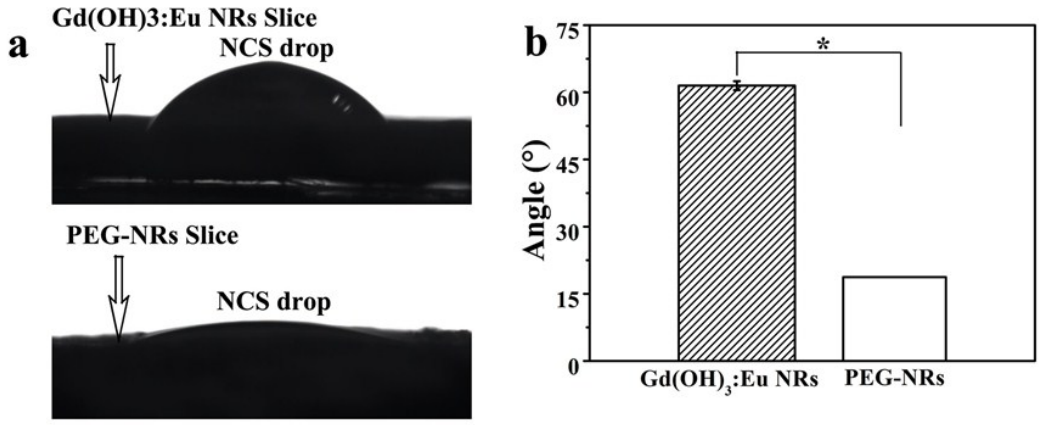

Fig. S13. Photographs of contact angle of NCS with $Gd(OH)_3$:Eu NRs slice and PEG-NRs slice (a), and the quantitative results of contact angle (b) before and after the conjugation of the hydrophilic dual-functional copolymer PEG.

In vivo hemolytic assay was usually used to investigate the interaction between nanomaterials and blood components.[2, 3] As shown in Fig. S14, the percentage of hemolysis upon the treatment of both $Gd(OH)_3$:Eu NRs and PEG-NRs with different concentrations were not higher than 50 % (even at the maximal experimental concentration of 1000 μg/mL), and the hemolytic rates of PEG-NRs of higher concentrations (250 ~ 1000μg/mL) was lower than that of corresponding $Gd(OH)_3$:Eu NRs, indicating the lower hemolysis rate, better biocompatibility of PEG-NRs and their feasibility for further in vivo investigation.

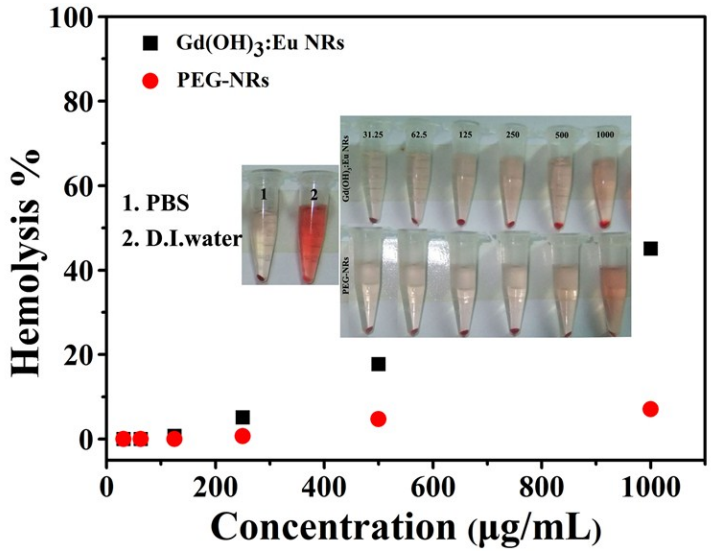

Fig. S14. The concentration-dependent hemolysis of $Gd(OH)_3$:Eu NRs and PEG-NRs, using double-distilled water as a positive control group and PBS as a negative control group. Inset: photographic images for direct observation of hemolysis.

In vitro cellular compatibility investigations were performed to assess the cytotoxicity of $Gd(OH)_3$:Eu NRs and RGD-NRs upon L929, HUVEC, and U251 cells. Fig.S15, S17, and S18 showed the photomicrographs of L929, HUVEC, and U251 cells after being treated for 1 d with $Gd(OH)_3$:Eu NRs and RGD-NRs suspension at different concentration. In Fig.S15, the treatment of 25 ~ 200 $\mu g \cdot mL^{-1}$ $Gd(OH)_3$:Eu NRs and RGD-NRs, cell were not changed remarkable in the morphology and the density. The number of cells was not reduced significantly compared with the control group. These results revealed that the treatment of pure NRs and RGD-NRs did not produce significant effect on L929 cells. MTT results in Fig. S16 showed the L929 surviving fraction in the different $Gd(OH)_3$:Eu NRs and RGD-NRs suspensions. When the cells were cultured with NRs for 24 h, both $Gd(OH)_3$:Eu NRs and RGD-NRs could promote the viability of cells at concentrations of 25 ~ 200 $\mu g \cdot mL^{-1}$, because metal ions at low concentration could promote the growth of cells.[4] As shown in Fig. S17 and S18, with the treatment of 25 ~ 50 $\mu g \cdot mL^{-1}$ $Gd(OH)_3$:Eu NRs and RGD-NRs, cell were hardly changed in the morphology and the density. Only some cells became round and were destroyed in the visual field. The number of cells was also not reduced significantly compared with the control group. However, both the treatment of $Gd(OH)_3$:Eu NRs and RGD-NRs of a higher concentration (100 and 200 $\mu g \cdot mL^{-1}$) produced a great deal of extra material deposited on the cells and "mechanically" induced extra stress to damage the cells. Meanwhile, $Gd(OH)_3$:Eu NRs and RGD-NRs in the treatment of 100 ~ 200 $\mu g \cdot mL^{-1}$ agglomerated seriously around the cells because of the hydrophilic nature of the NRs. Especially, RGD-NRs of high concentration of 200 $\mu g \cdot mL^{-1}$ produced negative effect on U251 cells, and only less normal cells could be observed in Fig.S18e.

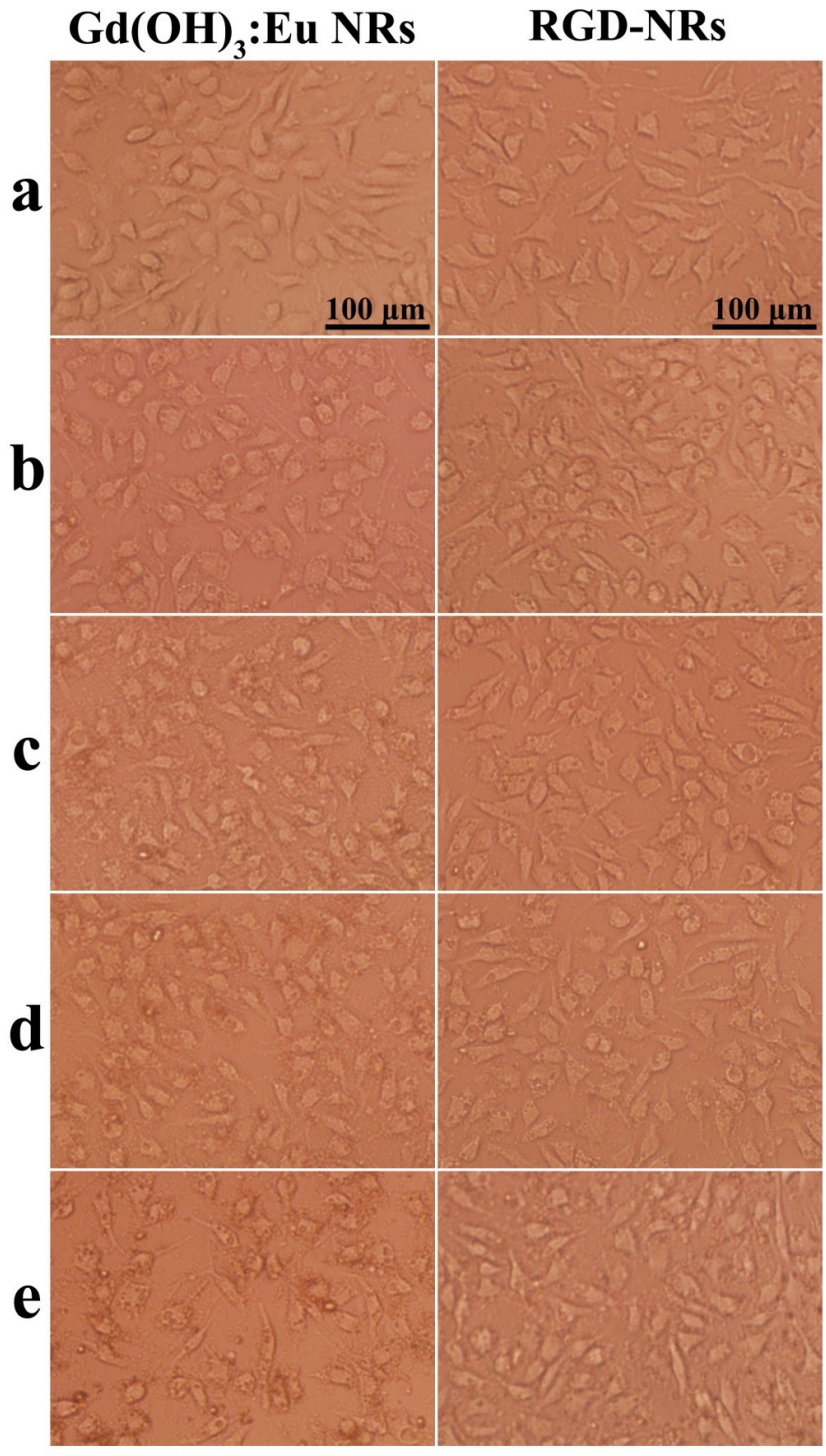

Fig. S15. The cellular morphology of L929 cells incubated with $Gd(OH)_3$:Eu NRs and RGD-NRs with different concentrations for 1 d (a) 0 μg/mL; (b) 25 μg/mL, (c) 50 μg/mL, (d) 100 μg/mL and (e) 200 μg/mL.

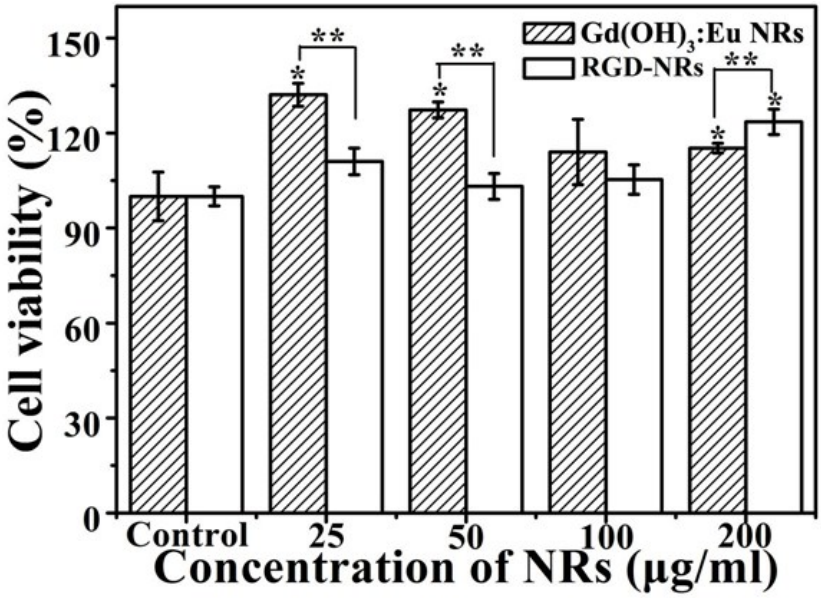

Fig. S16. In vitro cell viability of L929 cells incubated with $Gd(OH)_3$:Eu NRs and RGD-NRs with different concentration for 1 d (* shows significant difference with control group, ** shows significant difference between two corresponding groups, $p < 0.05$, $n = 3$).

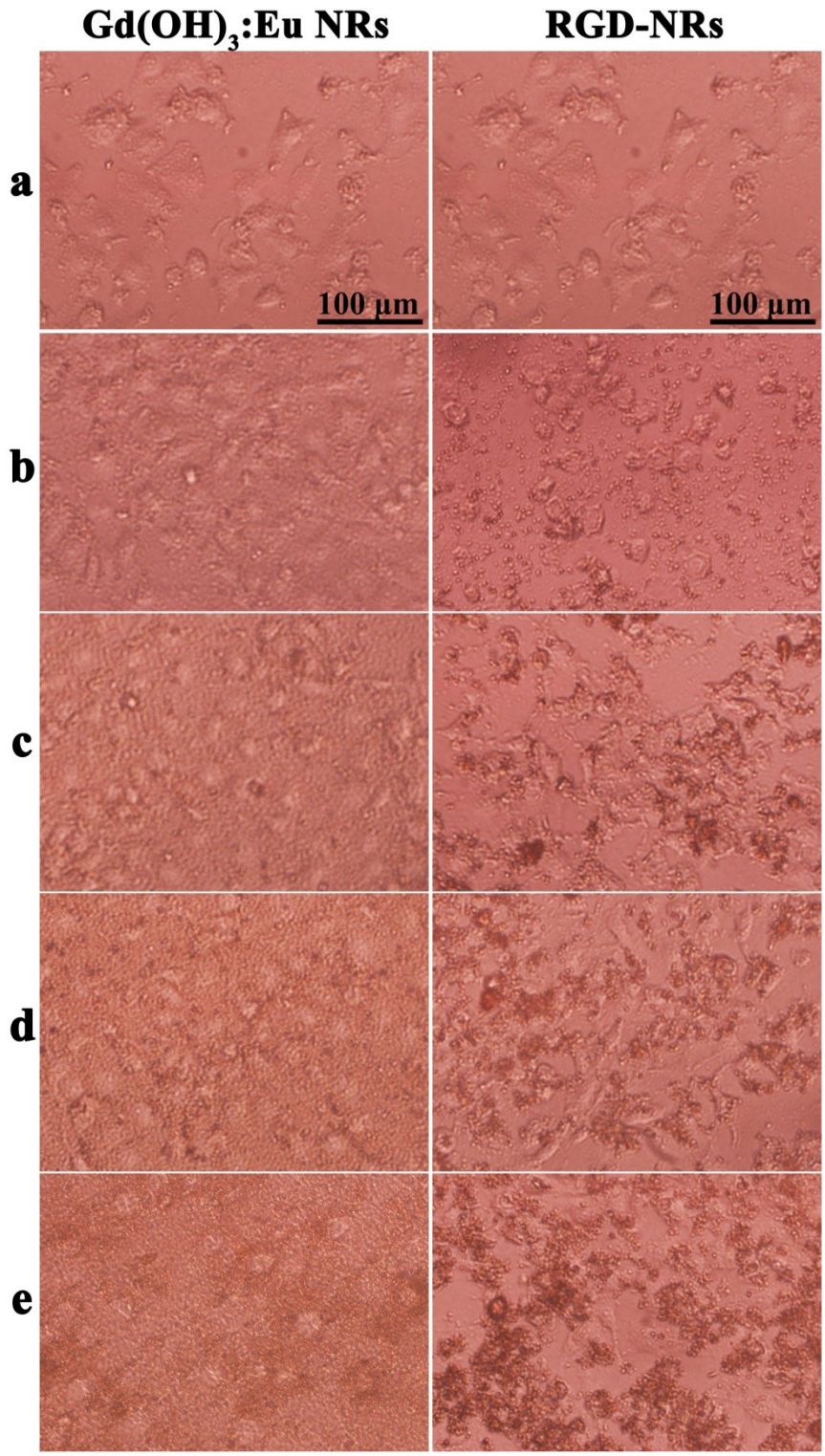

Fig. S17. The cellular morphology of HUVEC cells incubated with $Gd(OH)_3$:Eu NRs and RGD-NRs with different concentration for 1 d (a) 0 μg/mL, (b) 25 μg/mL, (c) 50 μg/mL, (d) 100 μg/mL and (e) 200 μg/mL.

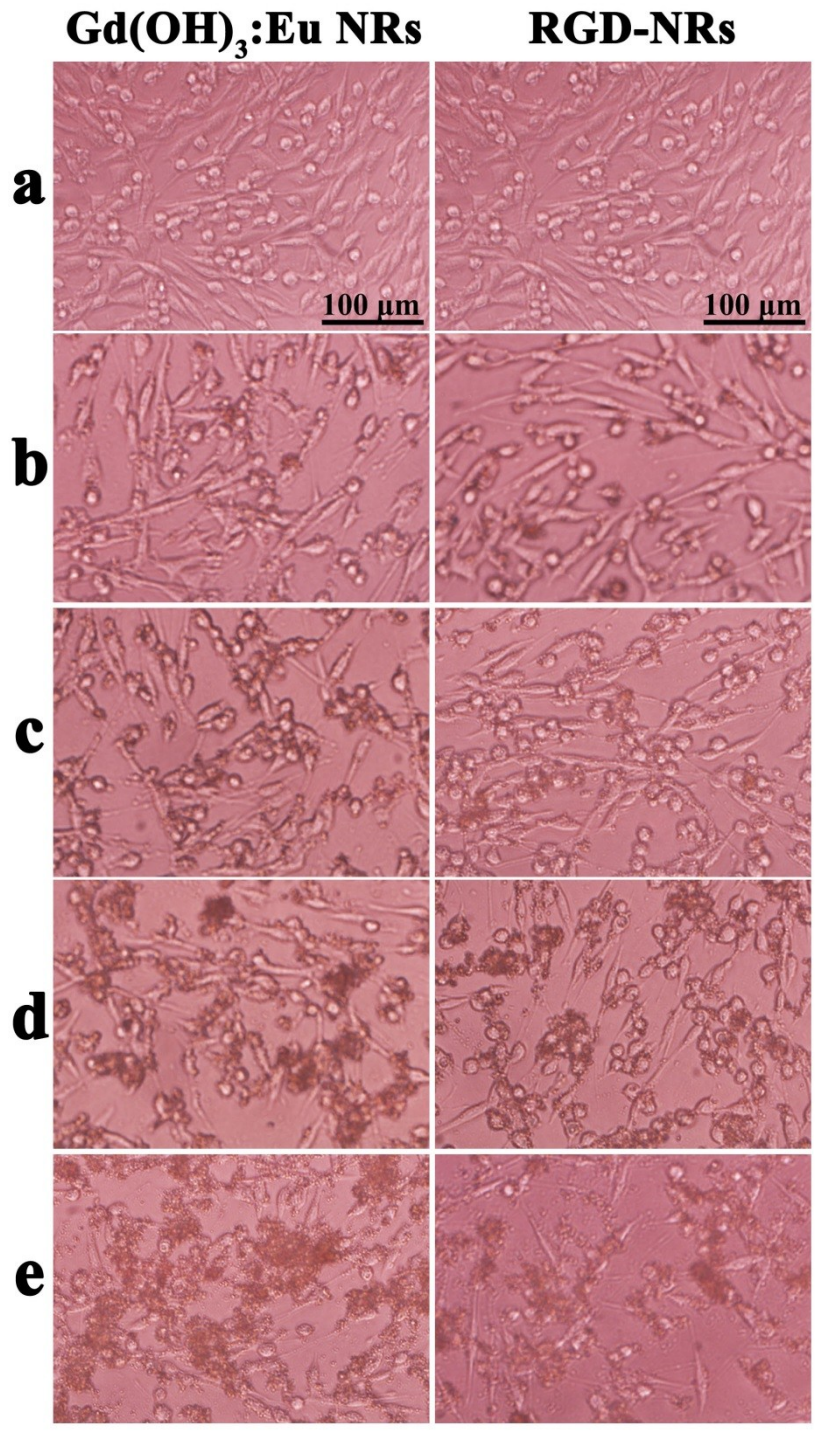

Fig. S18. The cellular morphology of U251 cells incubated with $Gd(OH)_3$:Eu NRs and RGD-NRs with different concentration for 1 d (a) 0 μg/mL, (b) 25 μg/mL, (c) 50 μg/mL, (d) 100 μg/mL and (e) 200 μg/mL.

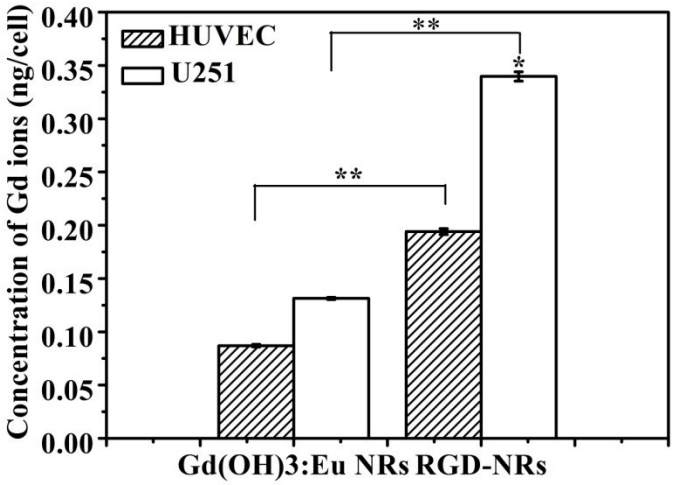

Fig. S19. The concentration of residual Gd ions in HUVEC and U251 cells incubated with $Gd(OH)_3$:Eu NRs and RGD-NRs for 24 h (* represents significant difference between two HUVEC cell groups incubated with RGD-NRs and ** shows significant difference between two corresponding NRs groups, $p < 0.05$, n=3).

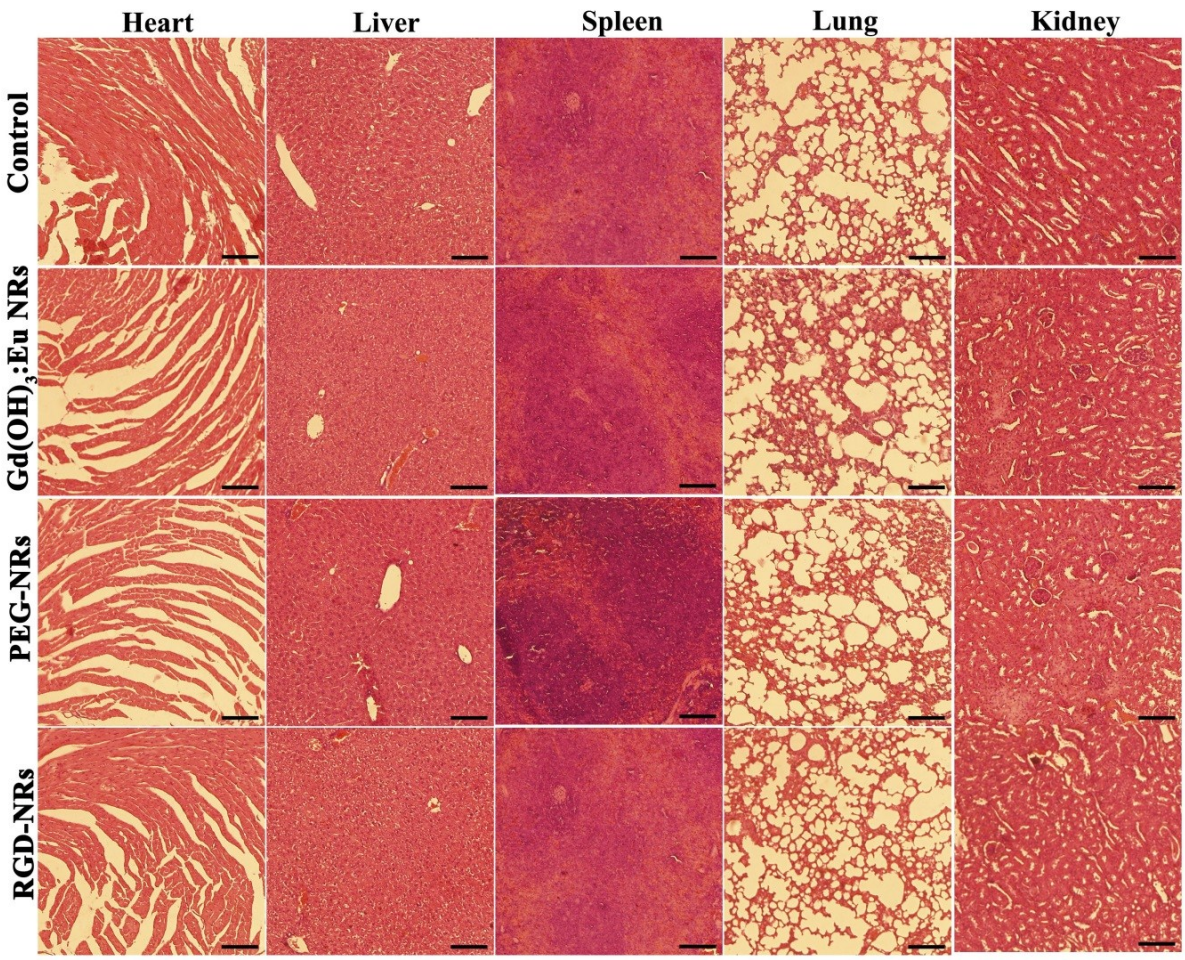

Fig. S20. Histological changes of the mice at 1 day after tail intravenous injection of different NRs solutions and the mouse without any NRs injection was selected as control group. These organs are stained with H&E and observed under a light microscopy. (scale bar is 100 μm).

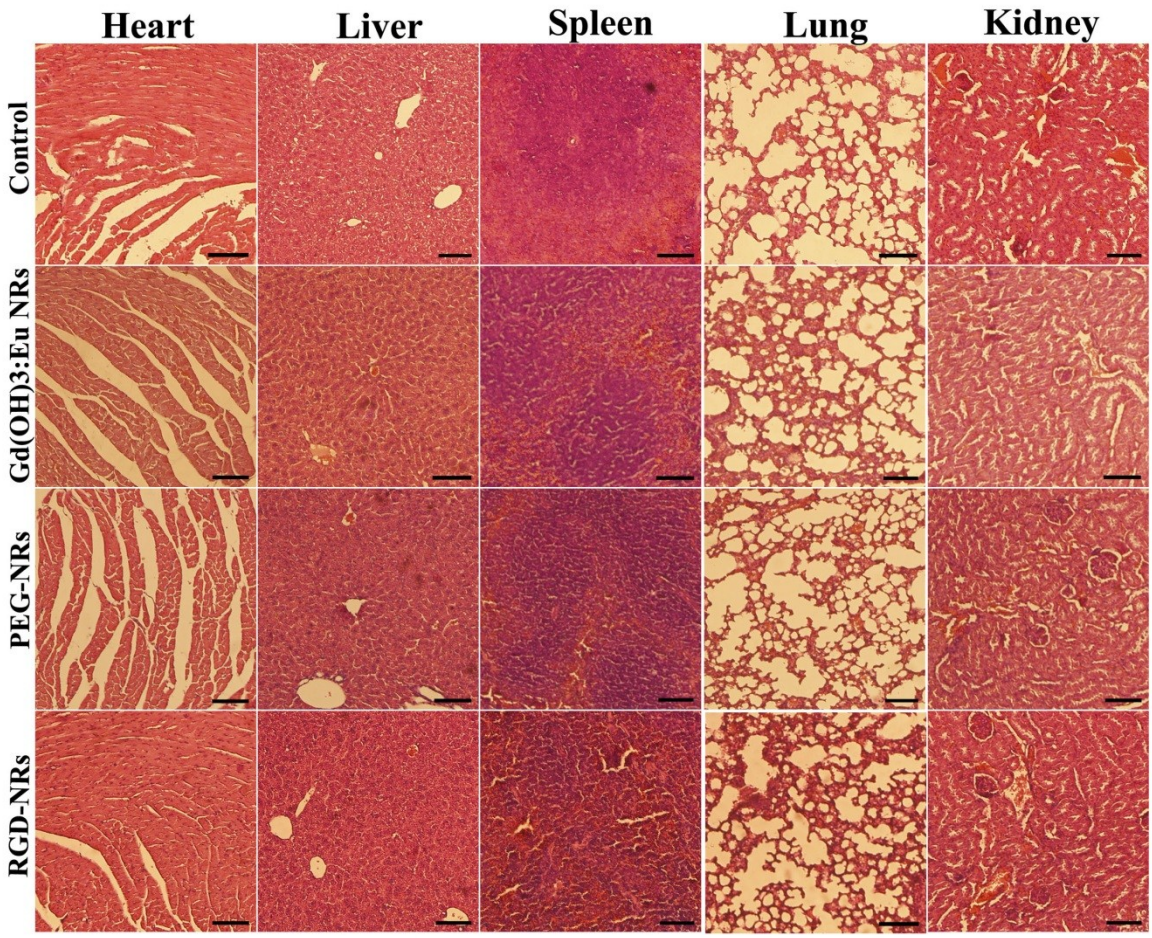

Fig. S21. Histological images of the mice at 10 days after tail intravenous injection of different NRs solutions, and the mouse without NRs injection was as control group. These organs are stained with H&E and observed under a light microscopy. (Scale bar is 100 μm).

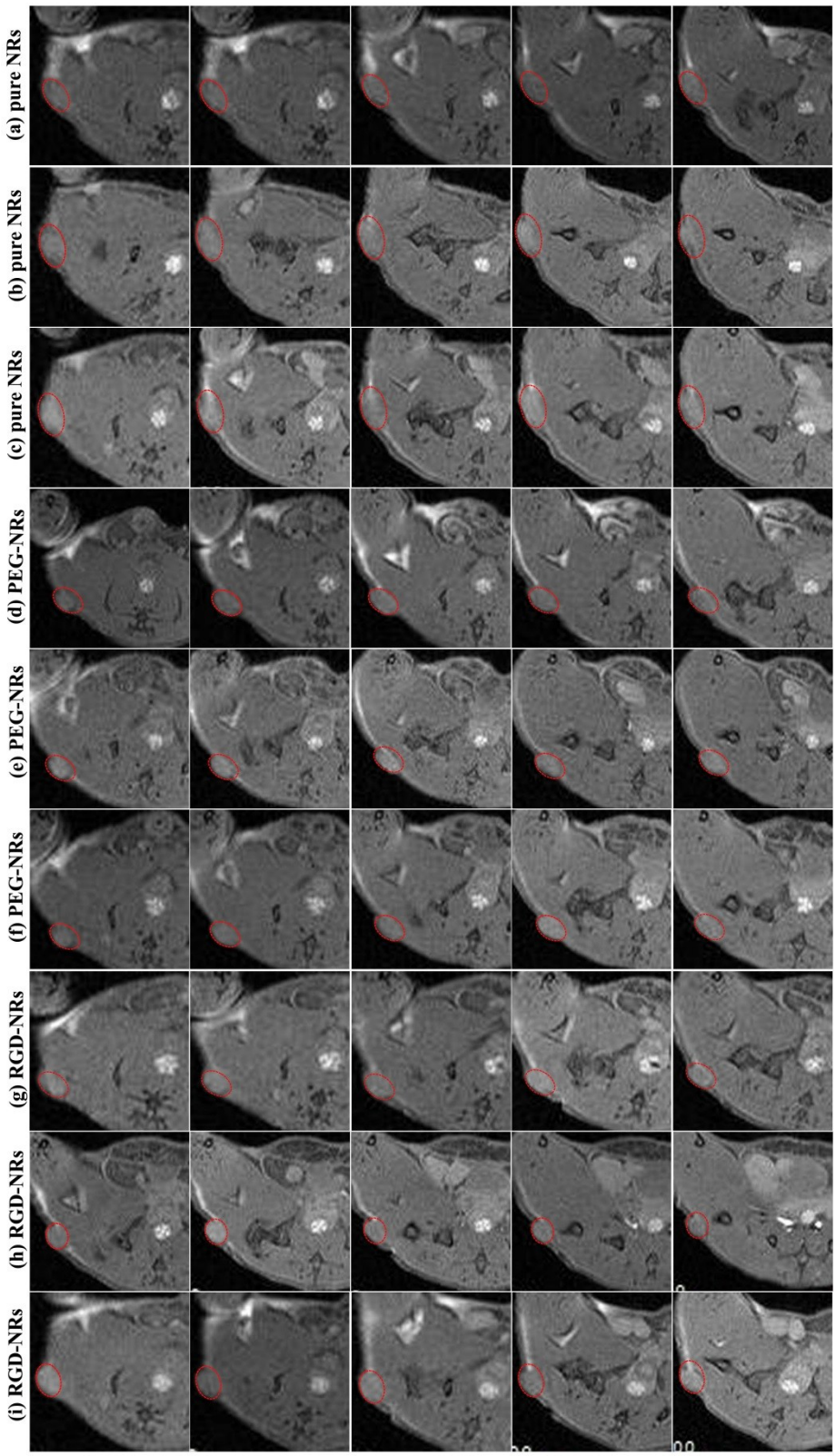

Fig. S22. In vivo T_1-weighted MR images of tumor-bearing mouse before (a, d, g) and 3 h (b, e, h), 24 h (c, f, i) after the injection of $Gd(OH)_3$:Eu NRs, PEG-NRs and RGD-NRs.

Table S3. The brightness of tumor interior and tumor periphery in a serial of MR images and the average intensity enhancement of tumor signal ($\Delta V = V_{\text{tumor interior}} - V_{\text{tumor periphery}}$) before and after 3 h, 24 h of the injection of $Gd(OH)_3$:Eu NRs, PEG-NRs and RGD-NRs.

NRs of injection	Time after injection (h)	Signal intensity of tumor site (V_1)	Signal intensity at the periphery of tumor(V_2)	Signal intensity enhancement ($\Delta V=V_1-V_2$)	Average of ΔV	standard deviation of ΔV
$Gd(OH)_3$:Eu NRs	0 h	82.3427	74.3095	8.0332	6.41948	3.13056
		83.5833	75.335	8.2483		
		84.3457	72.4197	11.926		
		66.7444	62.5579	4.1865		
		75.1311	70.4277	4.7034		
	3 h	98.4367	93.2253	5.2114	7.19785	4.10454
		95.2186	89.1079	6.1107		
		101.5433	91.034	10.5093		
		102.5951	91.6351	10.96		
		99.95165	90.7538	9.19785		
	24 h	109.2951	101.1669	8.1282	8.09098	2.71117
		110.3349	104.8782	5.4567		
		107.2004	95.1368	12.0636		
		101.5695	91.8541	9.7154		
		107.0171	98.3723	8.6448		
PEG-NRs	0 h	77.7615	74.0782	3.6833	6.26677	3.5307
		83.5523	78.7576	4.7947		
		97.2805	90.8845	6.396		
		108.0787	93.4834	14.5953		
		110.2826	98.6464	11.6362		
	3 h	101.623	88.8031	12.8199	12.44818	3.3568
		76.2427	63.9896	12.2531		
		96.0093	82.9338	13.0755		
		102.1669	88.3272	13.8397		
		126.311	115.8455	10.4655		
	24 h	99.3587	93.2253	6.1334	18.50425	4.83871
		103.2448	89.1079	14.1369		
		116.4015	91.034	25.3675		
		110.393	91.6351	18.7579		
		112.9061	90.7538	22.1523		

NRs of injection	Time after injection (h)	Signal intensity of tumor site (V_1)	Signal intensity at the periphery of tumor(V_2)	Signal intensity enhancement ($\Delta V=V_1-V_2$)	Average of ΔV	standard deviation of ΔV
RGD-NRs	0 h	104.6848	96.6833	8.0015	8.68657	3.5307
		95.9176	87.1656	8.752		
		113.0594	105.4837	7.5757		
		108.1515	99.3825	8.769		
		94.8702	87.014	7.8562		
	3 h	109.4002	101.1669	8.2333	20.10365	4.80688
		125.5496	104.8782	20.6714		
		113.4333	95.1368	18.2965		
		124.9143	91.8541	33.0602		
		121.9632	98.3723	23.5909		
	24 h	101.6491	79.6382	22.0109	31.40958	4.53769
		103.5957	76.4471	27.1486		
		122.8427	88.9602	33.8825		
		110.9223	75.5148	35.4075		
		111.7739	74.6272	37.1467		

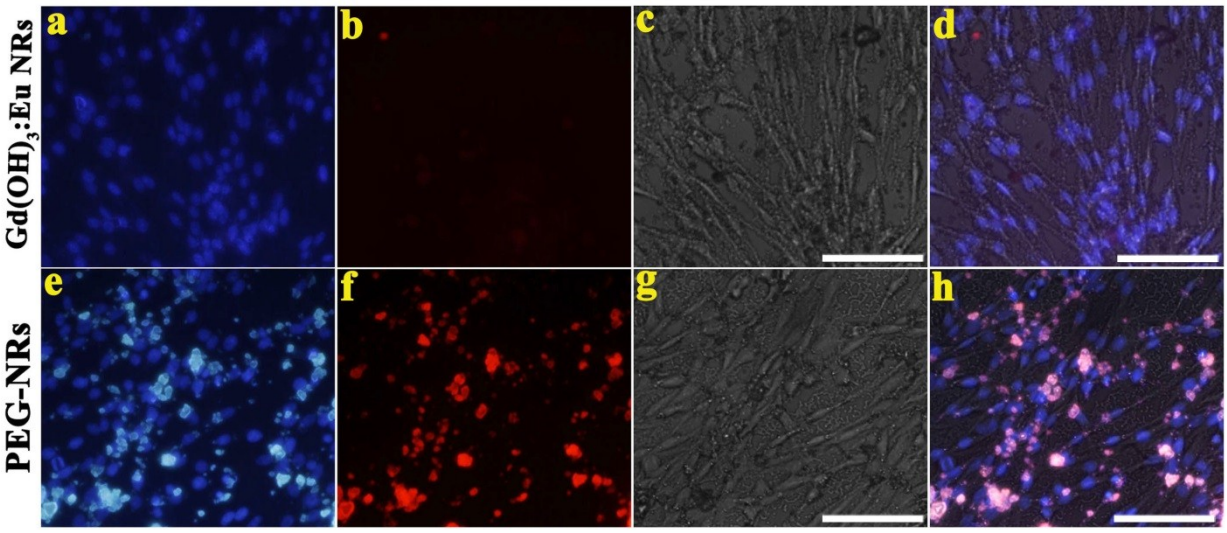

Fig. S23. The dark images (a, b, e, f) and the bright cellular images of U251 (c, g) and their corresponding overlapped images (d, h) of U251 cells co-cultured with $Gd(OH)_3$:Eu NRs and PEG-NRs for 24 h, respectively. (scale bar: 100 μm)

Reference

1 M. Bottrill, L. Kwok and N. J. Long, *Chem. Soc. Rev.,* 2006, **35**, 557.

2 Y.-S. Lin and C. L. Haynes, *J. Amer. Chem. Soc.,* 2010, **132**, 4834.

3 I. I. Slowing, C. W. Wu, J. L. Vivero‐Escoto and V. S. Y. Lin, *Small*, 2009, **5**, 57.

4 M. Deng, Z. Huang, Y. Zou, G. Yin, J. Liu and J. Gu, *Colloid. Surf. B: Biointerf.,* 2014, **116**, 465.